Proceedings of the 11th ICPMG 2026
11th International Conference on Physical Modelling in Geotechnics
8-12 June 2026, Zurich, Switzerland

Seismic Response of Embankments on Inclined Foundation under Liquefaction Conditions

W.-Y. Hung
National Central University, Taoyuan, Taiwan, wyhung@ncu.edu.tw

C.-H. Chen, M.-C. Tran
National Center for Research on Earthquake Engineering, National Institutes of Applied Research (NIAR), Taipei, Taiwan, chiaham@narlabs.org.tw, mctran@narlabs.org.tw

M.-C. Tran
Civil Engineering Faculty, Mien Tay Construction University, Vinh Long, Vietnam tranminhcanh@mtu.edu.vn

ABSTRACT: Embankments are critical components of infrastructure systems, serving as road platforms and flood protection barriers. However, they are often severely damaged under seismic loading, particularly when constructed on liquefiable soils. This study investigated the failure behavior of embankments subjected to earthquake-induced liquefaction through a series of centrifuge shaking table tests. Two foundation conditions were considered: horizontal and inclined base foundations. The shaking input had a frequency of 1 Hz with a peak base acceleration of 0.25 g. Test results show that the difference in settlement between horizontal and inclined foundations was minimal, suggesting that foundation inclination exerted only a limited influence on liquefaction-induced deformation. These findings underscore the critical role of soil saturation and liquefaction in governing embankment performance during earthquakes and provide valuable insights for the development of earthquake-resilient design strategies.

1 INTRODUCTION

Earthquake-induced soil liquefaction poses a significant threat to embankments founded on saturated loose sand deposits, often resulting in excessive settlement, lateral spreading, and structural failure. Understanding the deformation mechanisms of embankments subjected to foundation liquefaction is therefore essential for improving seismic design and mitigation strategies.

Previous physical model studies, including 1 g shaking table tests and centrifuge model tests, have provided important insights into embankment behavior under seismic loading. Koga et al. (1990) demonstrated that stress conditions beneath embankments differed significantly from free-field conditions, leading to distinct pore pressure responses and deformation patterns. Centrifuge investigations by Adalier et al. (1998) and Okamura et al. (2002) further revealed that embankment settlement was governed by multiple mechanisms, including lateral spreading of liquefied foundation soil, shear deformation within the embankment body, and volumetric compression at the base. More recent studies have shown that mitigation measures such as partial desaturation (Tomida et al., 2015) and reinforcement using geosynthetics (Hung, 2015) can effectively suppress excess pore pressure buildup and reduce settlement.

Despite these advances, the coupled interaction between liquefaction, lateral deformation, and embankment settlement under varying seismic intensities remains incompletely understood. Therefore, this study investigates the deformation behavior of embankments founded on liquefiable sand through physical modeling, with emphasis on excess pore pressure evolution and settlement mechanisms.

2 CENTRIFUGE MODELING

2.1 Configuration

This study used a geotechnical centrifuge and shaking table from National Central University to conduct a series of dynamic centrifugation model tests. These tests simulated a 3 m high earthen embankment with a bottom contact stress of approximately 60 kPa situated on a 12.5 m thick soil layer with a relative density of 55%. Two test groups were conducted: one with a horizontal foundation

(SFE) and the other with an inclined foundation (SIE) in Figure 1.

During the vibration of the specimen, various physical quantities were measured using different sensors, including the ground acceleration duration at different depths and locations, the acceleration duration of the embankment, the excess pore water pressure duration at different depths and locations, the vertical settlement of the embankment and the free field, and the horizontal displacement of the laminated test chamber.

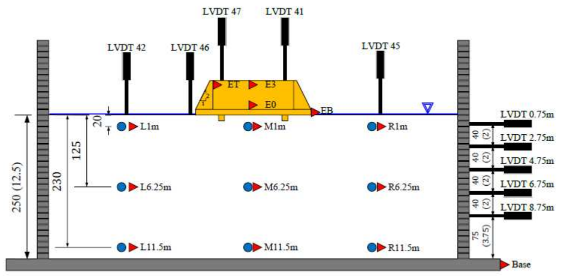

a) Embankment with a horizontal foundation (SFE)

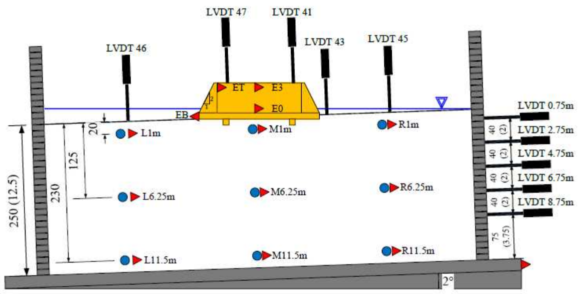

b) Embankment with an inclinition foundation (SIE)

Figure 1. Test configuration

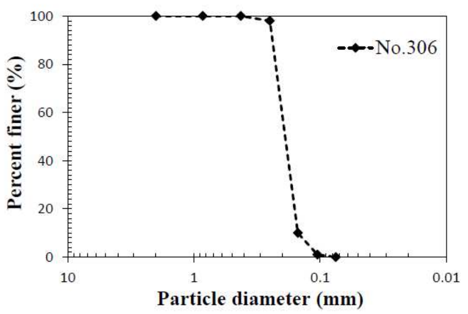

Figure 2. Test material

2.2 Material

The sand used in this study was 306 quartz sand from the Taiwan branch of Sibelco Asia Ltd., a Singapore-based company. The maximum and minimum dry densities were determined according to the method recommended by JSF T26-81T, with maximum and minimum dry unit weights of 16.3 kN/m³ and 14.1 kN/m³, respectively. The specific gravity (G_s) was 2.65, and the internal friction angle at 55% relative density was 35.7°. The particle size distribution curve is shown in Figure 2. The average particle size (D_{50}) was 0.19 mm, and the effective particle size (D_{10}) was 0.15 mm. In the Unified Soil Classification System, it is classified as poorly graded sand (SP). Additionally, the embankment was made by aluminum alloy.

2.3 Test procedure

In this study, sand model specimens were prepared using the air-pluviation (drop) method. A drop apparatus with a fixed drop height was adopted to ensure uniform specimen density. The preparation procedure is described as follows.

Prior to specimen preparation, the number and locations of embedded sensors were determined, including accelerometers and pore water pressure gauges. Permeable stones were prepared for the pore pressure transducers and allowed to cool to room temperature before assembly to ensure proper saturation and measurement accuracy. The assembled model test chamber was placed on a height-adjustable trolley and positioned directly beneath the steel delivery pipe. The distance between the pipe outlet and the specimen surface was carefully adjusted to maintain the predetermined drop height. During adjustment, care was taken to avoid bending or kinking of the flexible plastic tubing connected to the system. This distance was defined as the sand drop height.

The test sand was first sieved through a No. 20 sieve to remove oversized particles and ensure uniform gradation. The sieved sand was then poured into the funnel of the drop apparatus. Once an adequate quantity of sand was loaded, the steel pipe outlet was opened to initiate pluviation. A U-shaped loop deposition path was adopted to maintain a level soil surface and ensure a constant drop height during specimen formation. The thickness of each deposited layer was controlled to be within the diameter of the steel pipe. After completing each layer, the pipe outlet was closed, and the trolley was adjusted to restore the predetermined drop height. This procedure ensured a consistent relative density throughout the specimen. When the deposition reached designated elevations, accelerometers and pore water pressure gauges were installed. The sensor axes were aligned parallel to the longitudinal axis of the test chamber, and signal cables were securely fixed to prevent disturbance during subsequent deposition. Steps 3–5 were repeated until the sand layer reached the target height.

After completion, excess sand was carefully leveled and removed. The total weight of sand within the model chamber was measured using a crane scale, and the overall relative density of the sand layer was calculated.

3 TEST RESULTS

3.1 Input motions

A sine wave was used to simulate the seismic event, with a non-uniform sine wave with a frequency of 1 Hz, 15 periods, and a maximum input acceleration of approximately 0.25 g. Its waveform began with a small amplitude gradually increasing to a maximum amplitude, then gradually decreasing back to a small amplitude, as shown in Figure 3.

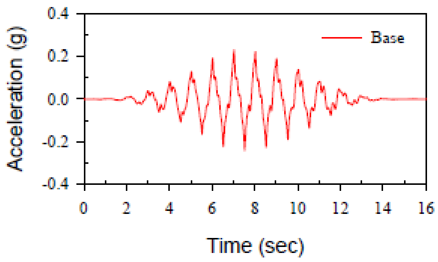

Figure 3. Input motion

3.2 Test results

The acceleration and excess pore water pressure ratio (r_u) time histories as shown in Figures 4 and 5. The base motion shows a relatively regular oscillatory pattern, while acceleration responses within the soil deposit were progressively modified with depth. In the upper layer (1 m), acceleration amplitudes were relatively small and attenuate rapidly as r_u increased, indicating stiffness degradation associated with pore pressure buildup. In the intermediate layer (6.25 m), r_u rose sharply and reached values close to or exceeding unity during shaking, accompanied by a noticeable reduction in acceleration amplitude and smoothing of high-frequency components, suggesting the onset of liquefaction and significant modulus reduction. In the bottom layer (11.5 m), r_u increased rapidly during shaking and approached unity, while acceleration initially amplified and then diminishes as effective stress decreases. Spatial differences among left, middle, and right locations were also evident, with variations in the timing of r_u buildup and acceleration attenuation, indicating non-uniform pore pressure development within the deposit. The excess pore water pressure on the left and right sides was generally similar at the same depth. However, a difference was observed between L1m and M1m, which may be attributed to the non-uniform stress distribution and soil deformation beneath the embankment during shaking. Under seismic loading, the embankment imposes an asymmetric surcharge on the foundation soil, altering the initial effective stress state and consequently influencing the development of excess pore water pressure.

Overall, the results demonstrated a strong coupling between acceleration response and excess pore pressure generation, where the progressive increase in r_u led to stiffness degradation.

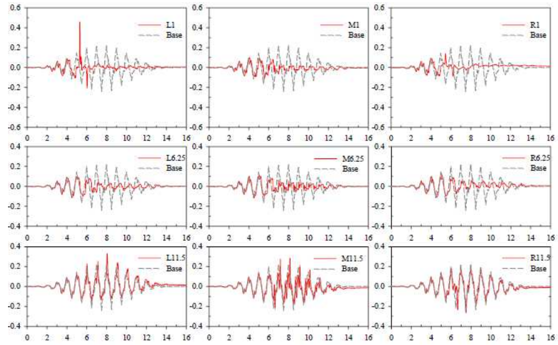

Figure 4. The acceleration time history of SFE

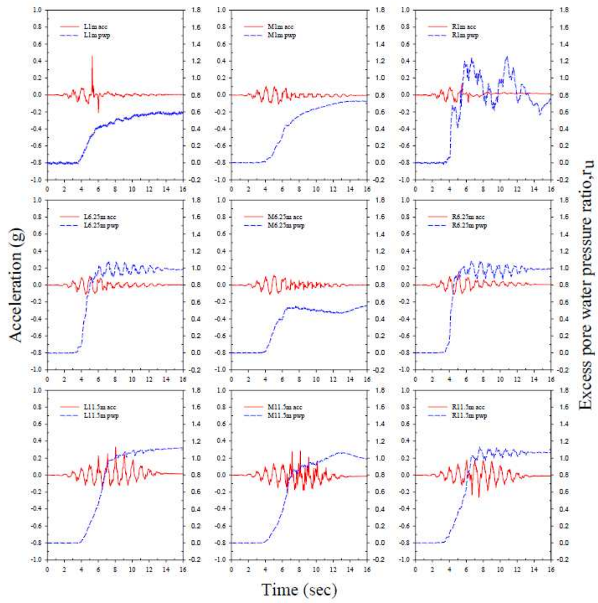

Figure 5. Excess pore water pressure ratio of SFE

In the SFE test, the short-term settlement induced by shaking was 0.412 m and 0.415 m at the left and right crest, respectively, 0.533 m at the embankment toe, and −0.048 m in the free field. The corresponding long-term settlements were 0.450 m (left), 0.460 m (right), 0.419 m (toe), and 0.090 m (free field). The differential settlement between the crest edges was only 0.01 m, resulting in a rotation angle of approximately 1/750, indicating nearly uniform settlement. The horizontal displacement was limited to 0.08 m, suggesting no lateral sliding occurred.

During shaking, excess pore water pressure buildup led to liquefaction and a temporary loss of bearing capacity, causing significant immediate subsidence of the embankment. Simultaneously, compression of the underlying soil induced slight heave in the adjacent free field. After shaking, additional long-term settlement occurred due to dissipation of excess pore water pressure and soil reconsolidation. The slight decrease in settlement measured by LVDT46 after shaking is attributed to temporary soil rebound during excess pore pressure dissipation and stress redistribution in the liquefied foundation layer. As the effective stress gradually recovers after shaking, partial elastic rebound may occur locally. In addition, interaction between embankment settlement and free-field heave adjacent to the embankment can produce a small reduction in the measured displacement at this location.

In the SIE test, short-term settlements were 0.335 m and 0.318 m at the left and right crest, respectively, 0.296 m at the toe, and −0.167 m in the free field. Long-term settlements increased to 0.419 m (left), 0.394 m (right), 0.339 m (toe), and −0.103 m (free field). The crest differential settlement was 0.025 m (rotation ≈ 1/300), indicating nearly uniform vertical deformation. However, horizontal displacement reached 1.00 m, confirming significant lateral spreading. Time histories show that liquefaction during shaking caused immediate settlement and free-field heave, followed by additional post-shaking settlement due to excess pore pressure dissipation and soil reconsolidation.

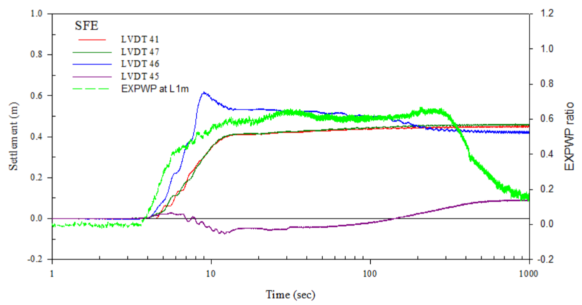

a) SFE - Test

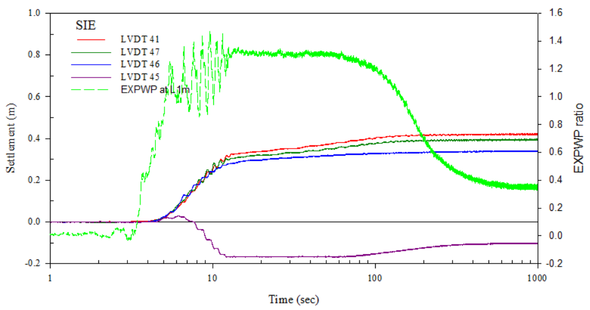

b) SIE - Test

Figure 6. The settlement during shaking event

4. CONCLUSIONS

The experimental results demonstrate that ground saturation plays a dominant role in controlling embankment settlement behavior. The settlements on saturated horizontal and inclined foundations (0.45 m and 0.42 m) were approximately 10–15 times greater than those on dry sand conditions (0.05 m and 0.03 m), confirming that liquefaction significantly amplifies vertical deformation. In contrast, ground inclination had limited influence on vertical settlement, as similar settlement magnitudes were observed for both horizontal and inclined configurations. After shaking, the embankments exhibited largely uniform settlement, with minimal differential deformation (maximum 0.01 m) and small rotation (approximately 1/300). However, lateral displacement behavior differed markedly. While negligible horizontal movement (approximately 0.10 m) occurred on dry or saturated horizontal ground, significant lateral spreading (~1.00 m) developed on saturated inclined ground following liquefaction, indicating that slope geometry primarily affects lateral stability rather than vertical settlement. Overall, liquefaction governs settlement magnitude, whereas ground inclination controls the potential for lateral slippage.

ACKNOWLEDGEMENTS

The authors are grateful for the financial support provided by the National Center for Research on Earthquake Engineering (NCREE), National Institutes of Applied Research (NIAR), Taipei, Taiwan.

REFERENCES

Koga, Y. and Osamu, M., "Shaking table tests of embankments resting on liquefiable sandy ground," *Japanese Society of soil Mechanics and Foundation Engineering*, Vol. 30, No. 4, pp. 162-174 (1990).

Adalier, K., Elgamal, A.W., Martin, G.R., "Foundation liquefaction countermeasures for earth embankment," *Journal of Geotechnical and Geoenvironmental Engineering*, Vol. 124, No. 6, pp. 500-517 (1998).

Okamura, M. and Osamu, M., "Effects of remedial measures for mitigating embankment settlement due to foundation liquefaction," *International Journal of Physical Modelling in Geotechnical*, Vol. 2, pp. 1-12 (2002).

Tomida, Y., Okamura, M., "Verification of desaturation technique as a liquefaction countermeasure for existing embankments," *International Journal of Landslide and Environment*, Vol. 3 No.1-3, pp. 1-7 (2015).